SUPPORTING INFORMATION

Evidence for Hydroxyl Radical Generation During Lipid Peroxidation.

Mathieu Frenette and Juan C. Scaiano*

[†]*Department of Chemistry, University of Ottawa, Ottawa, Ontario K1N 6N5, Canada*

Experimental Details.

GC-MS Analysis.

The gas chromatogram (model 6890N) and the mass selective detector (model 5973) were from Agilent Technologies. The column was a DB-5 (30 m length, 0.32 mm I.D.).

The autoxidation of methyl linoleate (>99% Sigma, freshly opened ampoules) was carried out in a Lab-line shaker held at 37°C in the dark. All autoxidations were initiated by 2,2'-azo-bis-isobutyronitrile (AIBN, twice recrystallized) and HPLC-grade benzene was the solvent. Efforts were made to keep the system under air without allowing benzene to evaporate during the long reaction times. For this reason, larger than necessary volumes were oxidized in a long-neck, narrow-mouth, round-bottom flask that was fixed with a rubber septum and a narrow needle protruded the septum to replenish the system of air. Aliquots of 250μL were taken at different reaction times and were immediately added to 100μL of 0.25M Ph_3P in benzene (to reduce the hydroperoxides to alcohols). To detect the phenol generated during the reaction, this mixture was injected directly in the GC-MS taking care to by-pass the mass detection during the lipid regions, as the lipids are too concentrated and could damage the detector. To detect lipid oxidation products, this later solution was diluted to a total of 10mL with dichloromethane and analyzed by GC-MS.

The phenol was quantified by extracting m/z=94.2±0.5 from the Total Ion Chromatogram, integrating the corresponding peak, and comparing these results with a similarly analyzed calibration curve using an authentic standard.

A mass selective chromatogram (m/z=94.2) showing the growth of phenol (Figure S1) and a Total Ion Chromatogram (TIC) of the lipid regions taken from the diluted sample after 50h of reaction time (Figure S2) are shown below.

Benzene was selected as a probe over others available, such as DMSO, because of the simplicity of product analysis. DMSO under oxygen is a candidate for complex product mixtures.

Oxygen Uptake Measurements.

The oxygen uptake data was acquired on a home-built differential pressure sensor, which was a very generous gift from L. Ross C. Barclay of Mount Alison University in New Brunswick. The pressure difference between a sample containing the oxidizable lipid and AIBN is compared to a reference cell (same as sample but without lipid) by means of a pressure transducer. The pressure difference is converted to a voltage signal and analyzed by a computer. To quantify

oxygen uptake data, the cells were calibrated against reactions that have known oxygen uptake rates such as AIBN in styrene [Howard, J. A. *Adv. In Free Radical Chem.* **1972**, *4*, 49-173].

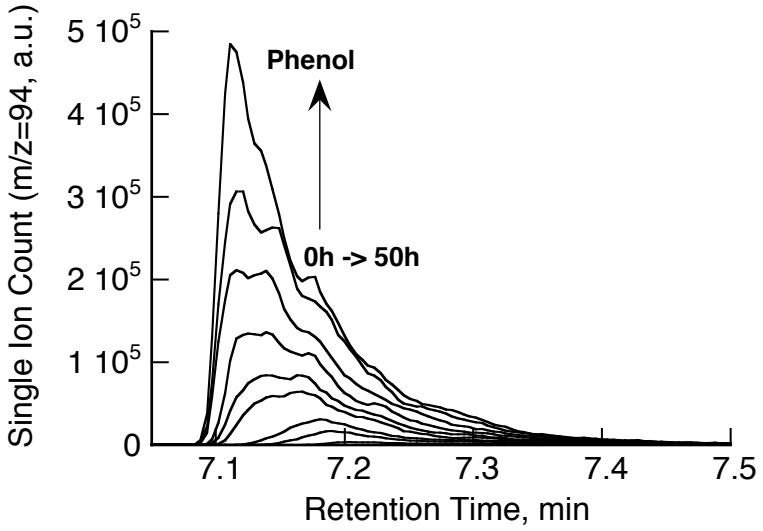

Figure S1. Mass selective chromatogram showing the growth of the phenol peak during the autoxidation of methyl linoleate by AIBN in benzene at 37ºC. The shift of the peak to shorter times was also observed during the calibration with the authentic sample.

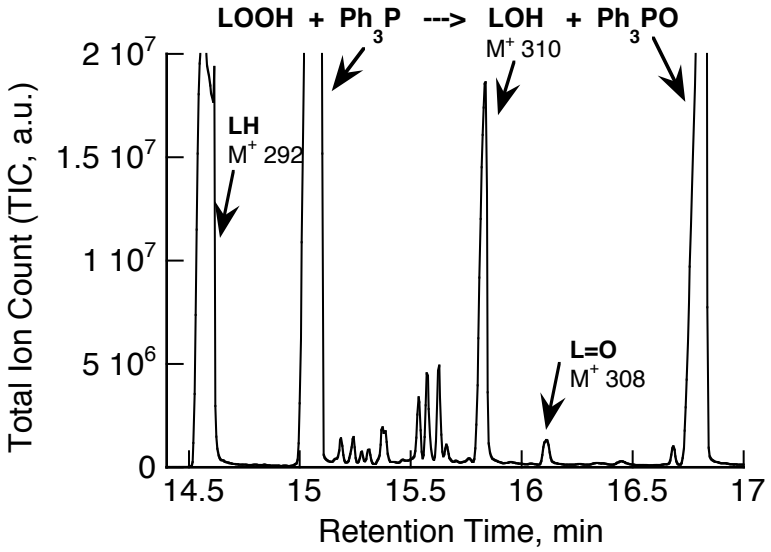

Figure S2. Total Ion Chromatogram for a diluted sample (see experimental details) of 0.189M methyl linoleate and 0.0189M AIBN after 50 hours at 37ºC under air. The peaks for **LOH** and **L=O** that were plotted in the paper (Figure 2) are indicated. The peaks corresponding to **LH**, **Ph_3P** and **Ph_3PO** are saturated at this concentration.

Peroxyl radical reactions with linoleate and its peroxide: which one is faster?

The following key reactions (Scheme S1) are competitive pathways for peroxyl radicals. The reactions are the same as appear in Schemes 1 and 2.
Computational chemistry suggests $\mathbf{k_A > k_B}$. The following analysis offers only a rough estimation, but confirms these relative values.

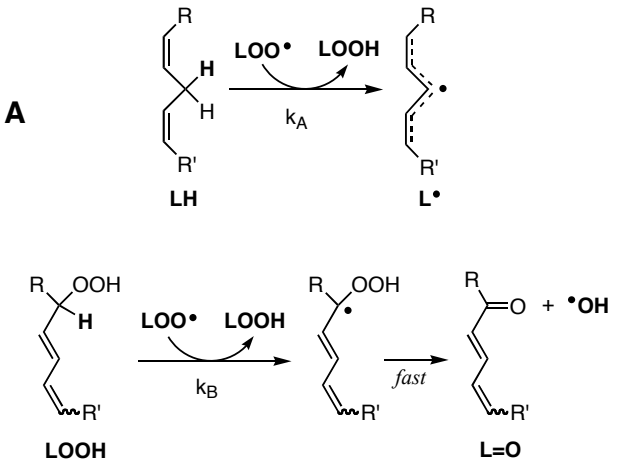

Scheme S1: reactions or peroxyl with LH and LOOH.

In order to estimate the relative values of $\mathbf{k_A}$ and $\mathbf{k_B}$ we perform the calculations after 20 h reaction at 37°C, thus ensuring a relative low conversion, yet enough accumulation of hydroperoxide to make reaction **B** a significant pathway. The rate of oxygen uptake can be determined from Figure 3, where the slope of the plot is 7.7×10^{-3} h^{-1}. When one takes into account that the LH concentration is 0.189 M (Figure 1, trace B), then the rate of oxygen uptake is 1.45×10^{-3} $M^{-1} h^{-1}$.
For phenol we base our analysis on curve B in Figure 1, where the tangent to the curve after 20h gives a slope of ~0.7×10^{-5} $M^{-1} h^{-1}$. Further, Figure 3 yield a conversion of 15% after 20 h; that is the ratio LH:LOOH is 85:15 after this time.

$$\frac{k_A}{k_B} \approx \frac{1.45 \times 10^{-3}}{0.7 \times 10^{-5}} \times \frac{15}{85} = 36.5$$

There is no doubt that this is a rough estimate, but accurate enough to conclude that reaction **A** is significantly faster than reaction **B**.

Computational Chemistry
Density Functional Theory calculations were performed using B3LYP (Becke's 3-parameter exchange [Becke, A. D. *J. Chem. Phys.*, **1993**, *98*, 5648] and Lee, Yang and Parr's correlation [C. Lee, W. Yang and R. G. Parr, *Phys. Rev. B*, **1988**, *37*, 785]) with a triple-ζ basis set (6-311+g(2d,2p)) as implemented in the Gaussian 03 software package.[S1] This level of theory was found satisfactory to estimate bond dissociation energies for lipid peroxidation reactions by Pratt, Mills and Porter [Pratt, D. A.; Mills, J. H.; Porter, N. A. *J. Am. Chem. Soc.* **2003**, *125*, 5801.] Transition states were confirmed by examining that only one imaginary vibrational frequency

corresponding to the reaction coordinate existed. The free energy surface of the reactions studied and the coordinate system for relevant structures are included below.
As reported before by Vereecken *et al*. for other similar radicals [L. Vereecken, L. T. Nguyen, I. Hermans, J. Peeters, *Chem. Phys. Lett.* **2004**, *393*, 432], the R_2C•OOH intermediate drawn in Scheme 2 does not have a barrier for the decomposition to the ketone and hydroxyl radical. It is possible that more refined computational approaches will reveal such a barrier, but it is unlikety that it will be high enough to prevent cleavage under ambient conditions.

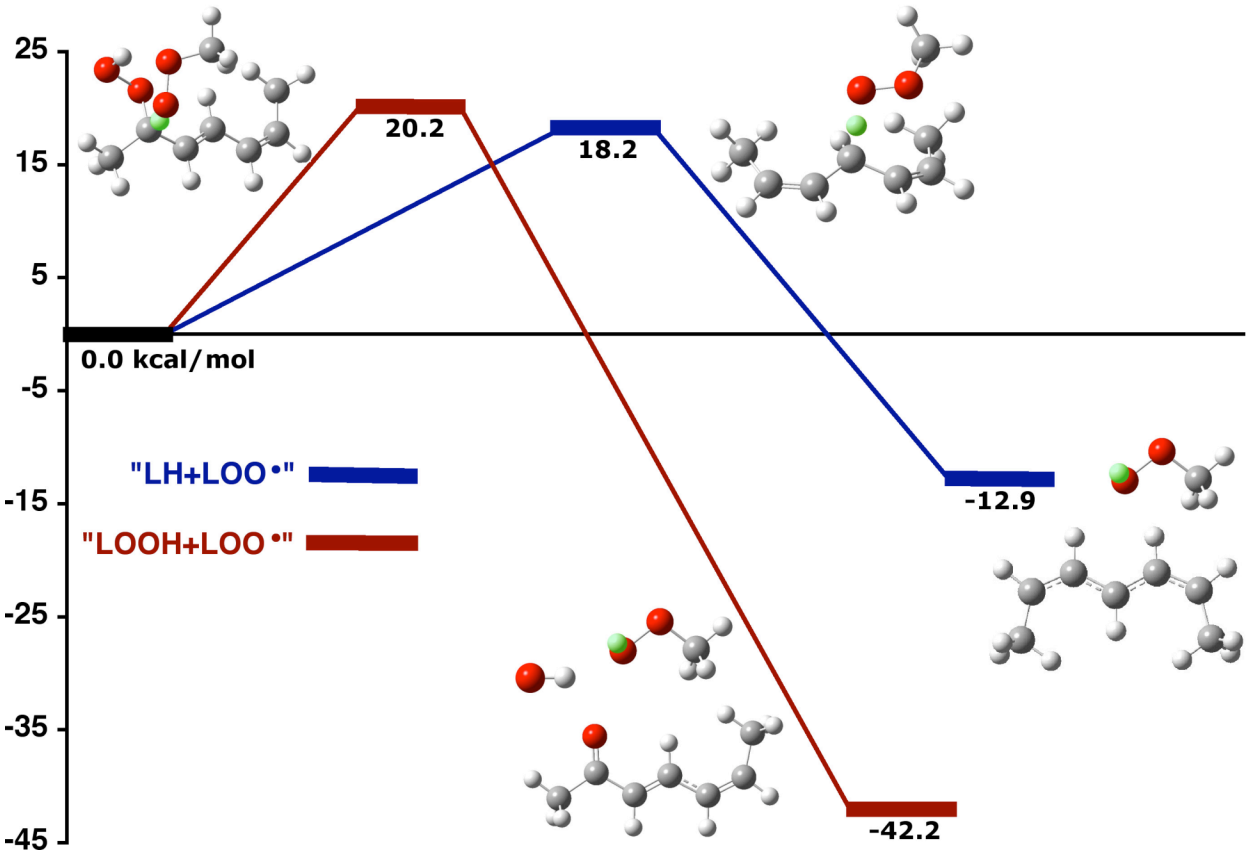

Figure S3. Calculated Free Energy Surface (298K, uncorrected) for the reaction of linoleate fragments, **LH** and **LOOH**, with a peroxyl radical, MeOO•, using the B3LYP/6-311+g(2d,2p) level of theory. "LH+LOO•" and "LOOH+ LOO•" correspond to the H-atom abstraction in schemes 1 and 2, respectively. The H-atom transferred is highlighted in green, other hydrogens are light grey, carbons are grey and oxygen atoms are red. The **LOOH** fragment shown in this figure has a *cis,trans* geometry; the *trans,trans* **LOOH** had similar thermodynamics (ΔG^{TS} = 20.3 kcal/mol and ΔG_{Rx} = -42.4 kcal/mol).

[S1] Gaussian 03, Revision B.04, Frisch, M. J.; Trucks, G. W.; Schlegel, H. B.; Scuseria, G. E.; Robb, M. A.; Cheeseman, J. R.; Montgomery, Jr., J. A.; Vreven, T.; Kudin, K. N.; Burant, J. C.; Millam, J. M.; Iyengar, S. S.; Tomasi, J.; Barone, V.; Mennucci, B.; Cossi, M.; Scalmani, G.; Rega, N.; Petersson, G. A.; Nakatsuji, H.; Hada, M.; Ehara, M.; Toyota, K.; Fukuda, R.; Hasegawa, J.; Ishida, M.; Nakajima, T.; Honda, Y.; Kitao, O.; Nakai, H.; Klene, M.; Li, X.; Knox, J. E.; Hratchian, H. P.; Cross, J. B.; Bakken, V.; Adamo, C.; Jaramillo, J.; Gomperts, R.; Stratmann, R. E.; Yazyev, O.; Austin, A. J.; Cammi, R.; Pomelli, C.; Ochterski, J. W.; Ayala, P. Y.; Morokuma, K.; Voth, G. A.; Salvador, P.; Dannenberg, J. J.; Zakrzewski, V. G.; Dapprich, S.; Daniels, A. D.; Strain, M. C.; Farkas,

O.; Malick, D. K.; Rabuck, A. D.; Raghavachari, K.; Foresman, J. B.; Ortiz, J. V.; Cui, Q.; Baboul, A. G.; Clifford, S.; Cioslowski, J.; Stefanov, B. B.; Liu, G.; Liashenko, A.; Piskorz, P.; Komaromi, I.; Martin, R. L.; Fox, D. J.; Keith, T.; Al-Laham, M. A.; Peng, C. Y.; Nanayakkara, A.; Challacombe, M.; Gill, P. M. W.; Johnson, B.; Chen, W.; Wong, M. W.; Gonzalez, C.; and Pople, J. A.; Gaussian, Inc., Wallingford CT, 2004.

"**LH**" fragment (*cis*,*cis*-2,5-heptadiene)

```
 E(UB+HF-LYP) =  -274.024389826
 Sum of electronic and zero-point Energies=          -273.854583
 Sum of electronic and thermal Energies=             -273.845624
 Sum of electronic and thermal Enthalpies=           -273.844680
 Sum of electronic and thermal Free Energies=        -273.889128
```

Atomic Number	Coordinates (Angstroms) X	Y	Z
6	2.319501	0.538338	-0.399512
1	2.878959	1.177987	-1.074953
6	1.004641	0.742598	-0.321773
1	0.579533	1.522575	-0.945006
6	3.143702	-0.475915	0.337173
1	3.898764	0.015216	0.956259
1	2.550187	-1.119715	0.982794
6	-1.004660	-0.742625	-0.321788
1	-0.579611	-1.522612	-0.945046
6	-2.319505	-0.538300	-0.399511
6	-3.143682	0.475944	0.337198
1	-2.550387	1.118587	0.984177
1	-3.899922	-0.015142	0.954867
1	-2.878984	-1.177879	-1.075005
6	0.000004	-0.000053	0.524162
1	-0.507404	0.711196	1.178231
1	0.507443	-0.711359	1.178145
1	-3.683696	1.115833	-0.365069
1	3.685109	-1.114614	-0.365086

"**LH+MeOO•**" Transition State

```
 Imaginary Frequency: -1496.9027 cm-1
 E(UB+HF-LYP) =  -464.294211501 Hartree
 Sum of electronic and zero-point Energies=          -464.086075
 Sum of electronic and thermal Energies=             -464.072408
 Sum of electronic and thermal Enthalpies=           -464.071464
 Sum of electronic and thermal Free Energies=        -464.129004
```

Atomic Number	Coordinates (Angstroms) X	Y	Z
6	-3.051764	-0.310605	-0.306930
1	-3.883667	-0.554483	-0.958737
6	-1.894498	0.028942	-0.895028

1	-1.864339	0.017072	-1.979504
6	-3.339154	-0.400979	1.159362
1	-3.601724	-1.425861	1.434762
1	-2.497119	-0.099387	1.778268
6	0.300462	1.236931	-0.978883
1	0.262413	1.134152	-2.058283
6	1.203090	2.095534	-0.476231
6	1.460957	2.409541	0.964463
1	0.802207	1.872312	1.643267
1	1.340647	3.479346	1.153776
1	1.819309	2.636256	-1.186293
6	-0.627671	0.377948	-0.232229
1	-0.017777	-0.723760	-0.166732
1	-0.730074	0.633683	0.818402
1	2.492295	2.165125	1.234398
1	-4.197355	0.221517	1.424746
8	0.615386	-1.891918	-0.082868
8	1.907992	-1.669551	-0.519676
6	2.767167	-1.512031	0.609208
1	3.767464	-1.393023	0.195963
1	2.488770	-0.625909	1.180656
1	2.720394	-2.396967	1.243279

"**L•**" fragment (*cis*,*cis*-2,5-heptadienyl radical)

E(UB+HF-LYP) = -273.401605117 Hartree
Sum of electronic and zero-point Energies= -273.245450
Sum of electronic and thermal Energies= -273.236475
Sum of electronic and thermal Enthalpies= -273.235531
Sum of electronic and thermal Free Energies= -273.280389

Atomic Number	Coordinates (Angstroms) X	Y	Z
6	-2.487760	0.362146	0.000003
1	-3.330986	1.042995	0.000048
6	-1.238853	0.914909	0.000018
1	-1.187964	1.999528	0.000043
6	-2.828702	-1.093549	-0.000020
1	-3.431991	-1.351872	-0.875113
1	-1.950771	-1.735786	-0.000705
6	1.238853	0.914909	-0.000018
1	1.187964	1.999528	-0.000043
6	2.487760	0.362146	-0.000003
6	2.828702	-1.093549	0.000020
1	1.950770	-1.735786	0.000689
1	3.431977	-1.351875	0.875121
1	3.330986	1.042995	-0.000048
6	0.000000	0.239124	0.000000
1	0.000000	-0.842205	0.000000
1	-3.430830	-1.352172	0.875795
1	3.430844	-1.352169	-0.875787

"**LOOH**" fragment (6-hydroperoxy-*cis*,*trans*-2,4 -heptadiene)

```
 E(RB+HF-LYP) =  -424.436292853 Hartree
 Sum of electronic and zero-point Energies=          -424.258785
 Sum of electronic and thermal Energies=             -424.247534
 Sum of electronic and thermal Enthalpies=           -424.246590
 Sum of electronic and thermal Free Energies=        -424.296127
```

Atomic Number	Coordinates (Angstroms) X	Y	Z
6	3.231810	-0.187028	-0.426642
1	4.014656	-0.423312	-1.139341
6	1.971781	-0.468076	-0.789366
1	1.816483	-0.912105	-1.766943
6	0.769077	-0.241621	-0.006664
1	0.879903	0.198559	0.977723
6	3.704395	0.420043	0.857924
1	2.895980	0.646753	1.548883
6	-0.465349	-0.549207	-0.424194
1	-0.608421	-0.985848	-1.409065
6	-1.710776	-0.321890	0.377001
1	-1.457254	0.026714	1.380134
6	-2.606776	-1.552814	0.450948
1	-2.071147	-2.368236	0.935379
1	-2.897750	-1.878731	-0.547826
8	-2.546869	0.686008	-0.238238
8	-1.915209	1.975044	-0.061406
1	-1.386414	2.049573	-0.867993
1	4.251301	1.346587	0.665577
1	4.402189	-0.251181	1.365089
1	-3.507870	-1.333624	1.021492

"**LOOH+MeOO•**" transition state

```
 Imaginary Frequency: -1477.1609 cm-1
 E(UB+HF-LYP) =  -614.703999478 Hartree
 Sum of electronic and zero-point Energies=          -614.487320
 Sum of electronic and thermal Energies=             -614.471703
 Sum of electronic and thermal Enthalpies=           -614.470759
 Sum of electronic and thermal Free Energies=        -614.531861
```

Atomic Number	Coordinates (Angstroms) X	Y	Z
6	-1.545814	-0.414883	-0.196655
1	-1.455234	-0.043754	0.814844
6	-0.466068	-0.987399	-0.771709
1	-0.546666	-1.367314	-1.784195
6	0.858542	-1.135622	-0.172405

1	1.578778	-0.211794	-0.641789
6	1.620338	-2.407184	-0.511781
1	1.106782	-3.271737	-0.086316
1	2.629880	-2.366721	-0.114615
8	0.802730	-0.824143	1.202802
8	2.149006	-0.727106	1.730535
1	2.397736	0.170423	1.447044
1	1.673403	-2.528310	-1.592955
8	2.338224	0.765766	-1.137342
8	2.489582	1.650343	-0.064844
6	1.564491	2.731674	-0.213117
1	1.760677	3.393154	0.629361
1	1.749136	3.250767	-1.152513
1	0.538872	2.366492	-0.177487
6	-2.818873	-0.292154	-0.864910
1	-2.857324	-0.668175	-1.881860
6	-3.946417	0.235354	-0.353857
1	-4.818724	0.252028	-0.998109
6	-4.151551	0.806834	1.013091
1	-4.939185	0.262152	1.540273
1	-3.256158	0.778755	1.629115
1	-4.486201	1.845429	0.948056

"**L=O**" fragment (*cis*,*trans*-3,5-heptadien-2-one)

E(RB+HF-LYP) = -348.077261114 Hartree
Sum of electronic and zero-point Energies= -347.926384
Sum of electronic and thermal Energies= -347.916879
Sum of electronic and thermal Enthalpies= -347.915935
Sum of electronic and thermal Free Energies= -347.961494

Atomic Number	Coordinates (Angstroms) X	Y	Z
6	2.864331	-0.516559	0.000036
1	3.652549	-1.262001	0.000078
6	1.598462	-0.968035	-0.000141
1	1.445221	-2.041654	-0.000219
6	0.405296	-0.154783	-0.000209
1	0.504406	0.923801	-0.000469
6	3.333543	0.902918	0.000132
1	3.959673	1.095459	-0.874805
1	2.521864	1.625535	0.000251
6	-0.846658	-0.645366	0.000075
1	-1.016991	-1.715925	0.000330
6	-2.033189	0.241681	0.000035
6	-3.384227	-0.443449	0.000093
1	-3.481762	-1.086393	-0.877570
1	-4.177069	0.298745	-0.000068
8	-1.938892	1.456861	-0.000071
1	-3.481853	-1.086200	0.877870
1	3.959763	1.095300	0.875038